

# Heterogeneity in the pyramidal network of the medial prefrontal cortex

Yun Wang<sup>1</sup>, Henry Markram<sup>2</sup>, Philip H Goodman<sup>3</sup>, Thomas K Berger<sup>2</sup>, Junying Ma<sup>1</sup> & Patricia S Goldman-Rakic<sup>4,5</sup>

The prefrontal cortex is specially adapted to generate persistent activity that outlasts stimuli and is resistant to distractors, presumed to be the basis of working memory. The pyramidal network that supports this activity is unknown. Multineuron patch-clamp recordings in the ferret medial prefrontal cortex showed a heterogeneity of synapses interconnecting distinct subnetworks of different pyramidal cells. One subnetwork was similar to the pyramidal network commonly found in primary sensory areas, consisting of accommodating pyramidal cells interconnected with depressing synapses. The other subnetwork contained complex pyramidal cells with dual apical dendrites displaying nonaccommodating discharge patterns; these cells were hyper-reciprocally connected with facilitating synapses displaying pronounced synaptic augmentation and post-tetanic potentiation. These cellular, synaptic and network properties could amplify recurrent interactions between pyramidal neurons and support persistent activity in the prefrontal cortex.

Working memory is the ability to keep information immediately available for a period of time in order to solve a task that may be delayed; it is therefore a fundamental component of higher cognitive functions<sup>1,2</sup>. The prefrontal cortex (PFC) has been identified as the key neocortical region supporting working memory<sup>3</sup>. Extracellular recordings in the prefrontal cortex during delayed response tasks have shown that a large fraction of prefrontal cortical neurons remain active after the cue and until the task is completed. Such activity can persist for several seconds without continued stimulation and has been proposed as the neural correlate of working memory<sup>1,2,4</sup>. Although persistent activity can be observed in other parts of the neocortex, it is found less frequently and does not seem to be as insensitive to interference from distractors as the activity in the PFC (refs. 1,2). The PFC therefore seems adapted to produce a robust form of persistent activity.

Different theories have been proposed to explain how the PFC generates persistent activity. One possibility is that reverberations in long-range loops between the PFC and thalamus and several other brain regions sustain this activity (see reviews in refs. 4,5). Another possibility is that the recurrent microcircuitry in the PFC intrinsically supports persistent activity<sup>4,5</sup>. However, synaptic depression, which is common between pyramidal cells throughout the neocortex, makes it difficult to sustain active states. On the other hand, some evidence exists for synaptic augmentation in the medial prefrontal cortex (mPFC), mainly using extracellular stimulation<sup>6</sup>, but the anatomical and physiological features of the microcircuitry have not yet been

investigated. In particular, it is not known how pyramidal cells are interconnected to form the excitatory recurrent network in the PFC.

We therefore used multineuron patch-clamp recordings to study synaptic connectivity between layer 5 pyramidal cells in the mPFC of young adult ferrets. We also compared their properties with those in the visual cortex at the same age. We found a synaptic architecture in the mPFC with a heterogeneity of synaptic dynamics, notable facilitation, synaptic augmentation and post-tetanic potentiation (PTP) at many synaptic connections, and more than double the rate of reciprocal connections compared with visual cortex. Further, the different types of synapses primarily interconnected different types of pyramidal cells to form distinct subnetworks. One subnetwork, which was composed of morphologically simple pyramidal cells typical of primary areas with spike train accommodation, was interconnected with depressing synapses. Another subnetwork composed of complex pyramidal cells displaying nonaccommodating discharge behavior was heavily interconnected with facilitating synapses that also showed pronounced synaptic augmentation and PTP. We found three major classes of synapses, suggesting a third pyramidal subnetwork. By recording divergent and convergent connections, we also found that the mPFC pyramidal neurons can form different types of synapses within and across these subnetworks.

These results provide the first insight into the complex organization of the mPFC microcircuitry and reveal multiple cellular, synaptic and network features characterizing the connections between pyramidal cells that could be important for persistent activity.

<sup>1</sup>Division of Neurology Research, Caritas St. Elizabeth's Medical Center, Tufts University, Boston, Massachusetts 02135, USA. <sup>2</sup>Brain and Mind Institute, Ecole Polytechnique Fédérale de Lausanne (EPFL), Lausanne 1015, Switzerland. <sup>3</sup>Department of Internal Medicine and Program in Biomedical Engineering, University of Nevada, Reno, Nevada 89557, USA. <sup>4</sup>Department of Neurobiology, Yale University School of Medicine, New Haven, Connecticut 06510, USA. <sup>5</sup>Deceased. Correspondence should be addressed to Y.W. (yun.wang@tufts.edu).

Received 28 November 2005; accepted 21 February 2006; published online 19 March 2006; doi:10.1038/nn1670

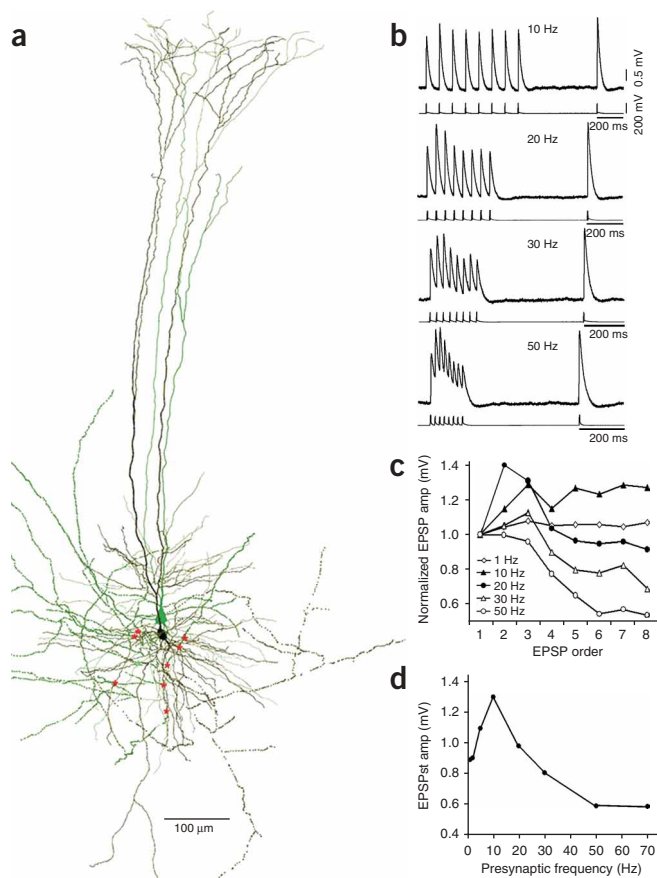


**Figure 1** Facilitating connections in the mPFC. **(a)** Computer reconstruction of a pair of synaptically connected layer 5 cPCs in the mPFC. Green, presynaptic cell; black, postsynaptic cell; red asterisks, putative synapses. **(b)** Synaptic responses of the long-lasting facilitation were recorded at different presynaptic frequencies from the connection in **a**. The recovery test responses remained further facilitated compared with the EPSP amplitudes during the train. The presynaptic action potential trace is presented under each EPSP trace. **(c)** Normalized EPSP amplitudes versus EPSP sequence during the time of presynaptic train. The steady state responses were gradually depressed as the presynaptic frequencies during the trains were increased. **(d)** Steady-state EPSP amplitudes versus presynaptic action potential frequencies, demonstrating frequencies of optimal responses (for this example, 10 Hz). Each point in **c** and **d** represents the average of 20–30 EPSPs of the connection in **a**.

Dynamic synaptic responses are due to the interplay between  $p$ ,  $D$  and the time constant of recovery from facilitation,  $F$ . To extract these parameters from the synaptic responses, we fitted the responses using a model of dynamic synaptic transmission<sup>9</sup>. Fitting the responses yielded these three parameters as well as the absolute strength,  $A$ , of the synaptic connection (defined as the response when  $p$  equals 1). In the model,  $U$  (utilization of synaptic resources) is used analogously to  $p$ . This model captures short-term synaptic dynamics with a high degree of accuracy using the appropriate set of four parameters,  $DFUA$  (example in **Fig. 2a**; amplitude fit in **Fig. 2b**). A model that fits the changing response amplitudes during train stimulation can extract  $F$ , but the facilitation can also be experimentally verified by lowering  $p$  using an extracellular perfusate with decreased calcium concentration ( $[Ca^{2+}]_{out}$  0.75 mM; **Fig. 2c**;  $n = 9$ ). We were surprised to find that these facilitating synapses had high release probabilities, as shown by the often strong initial responses (**Fig. 1b** and **Fig. 2a**). This was unexpected because facilitating synapses typically have rather low probabilities of release<sup>8,10–12</sup>. This indicates that, on average, functional facilitation in the mPFC is significantly masked by this high probability of release, which effectively results in synaptic depression. We found no difference in the degree of facilitation expressed at these synapses between the different ages from 1.5 to 3 months, indicating that the circuitry had largely stabilized (**Supplementary Fig. 1** online).

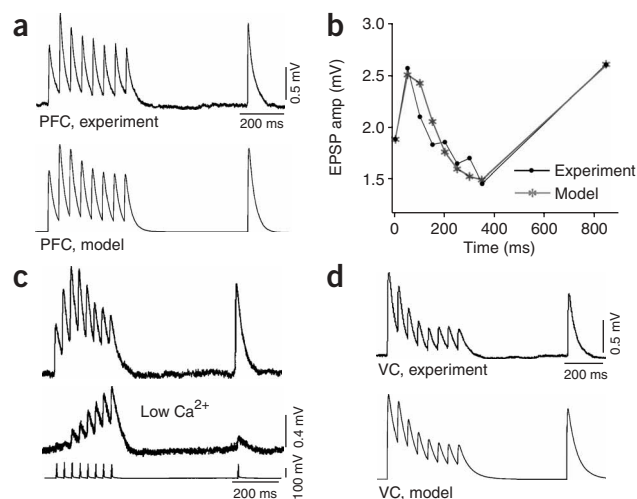
In contrast to the typical excitatory synapses in the mPFC, the typical connections in the visual cortex of ferrets of the same age showed only classical synaptic depression (**Fig. 2d**). When these rapidly depressing synapses were fitted using the model, most of them could be entirely explained without any facilitation at all. Only 4 of the 26 modeled

## RESULTS

### Synaptic facilitation in the mPFC

Triple patch-clamp recordings from layer 5 pyramidal cells ( $n = 1,233$  pairs, **Supplementary Table 1** online) in the mPFC (**Fig. 1a**) of young adult ferrets (1.5- to 3-months-old) revealed facilitating synaptic responses between pyramidal cells (**Fig. 1b**). Long-lasting facilitation was visually evident from the amplified response to the recovery test stimulus delivered 500 ms after a presynaptic train (6–8 action potentials); this was similar to the long-lasting facilitation seen in synapses onto some interneurons<sup>7,8</sup>. However, these facilitating synapses often presented a high initial probability of release ( $p$ ). This form of facilitation led to initial amplification before synaptic depression took over to limit transmission (**Fig. 1c**). The speed with which synaptic depression became dominant depended on  $p$  and on the time constant to recover from synaptic depression ( $D$ ); synaptic depression became more obvious as the presynaptic frequency increased (**Fig. 1d**). The amplitudes of synaptic responses of such synapses were maximal over a narrow range of ‘optimal’ frequencies (around 5–10 Hz, **Fig. 1d**), as apposed to the low-pass transmission of typical depressing synapses<sup>8</sup>.

**Figure 2** Recorded and modeled synaptic connections in the mPFC and visual cortex. **(a)** Examples of recorded (upper) and modeled (lower) traces in the mPFC. **(b)** Fit to the measured amplitudes between the experimental (black) and modeled (gray) traces in **a**. **(c)** Averaged EPSPs (30 traces) in standard (2 mM, upper trace) and lower  $[Ca^{2+}]_{out}$  (0.75 mM, lower trace). A classical facilitation was unmasked by reducing calcium concentration in the bath. The presynaptic action potential trace is presented under the EPSP traces. **(d)** Examples of recorded (upper) and modeled (lower) traces in the visual cortex. The synaptic responses represented classical depression.



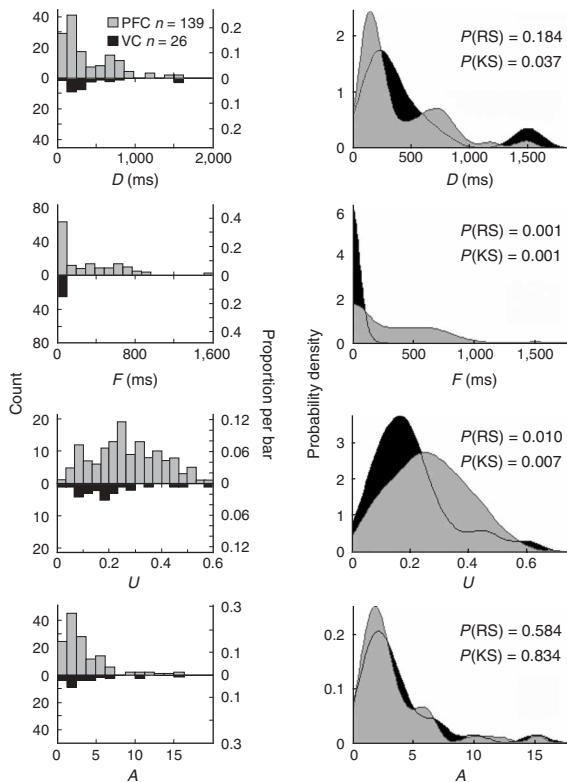


**Figure 3** Distribution of model parameters (*DFUA*) of all connections studied in the mPFC and visual cortex. Left, histograms for each parameter (*D*, depression time constant; *F*, facilitation time constant; *U*, utilization of synaptic resources; *A*, absolute strength). Upward bars: mPFC,  $n = 139$ ; downward bars: visual cortex,  $n = 26$ . Right, smoothed probability density functions (PDFs) of histograms. *P* values are for two-sided statistical comparisons of central tendency (RS, rank-sum test) and distribution shape (KS, Kolmogorov-Smirnov). PDFs highlight significant distributional discrepancies between the mPFC and visual cortex, suggesting multimodal clustering of *D* (especially midrange peak at about 750 ms) and the absence of a meaningful tail for *F* greater than 200 ms. See **Supplementary Methods** for details.

performed some experiments in the adult rat somatosensory cortex and observed facilitating synapses in this region (data not shown). Facilitating excitatory synapses are therefore not entirely unique to the mPFC; nonetheless, they seem to be a major feature of this region.

### A heterogeneity of synaptic dynamics

Although facilitating synapses dominate in this region of the mPFC, we also observed a spectrum of other synaptic dynamics. Synaptic dynamics are critically determined by the interactions between the parameters, and we therefore investigated tendencies for the *DFUA* parameters to cluster. The probability density functions for *DFUA* suggested some nonuniformity in the distribution of these parameters, which were significantly different in Kolmogorov-Smirnov tests (**Fig. 3**).

We used quality threshold clustering (QTC) to cluster the *DF* combinations. QTC is an unsupervised clustering algorithm that does not prespecify the number of clusters and uses jack-knife validation to ensure that synapses do not fall into a cluster because of only one or two parameters (**Supplementary Methods** online). QTC showed three major clusters, characterized by  $F \gg D$  (facilitation-dominant synapses, E1 type),  $D \gg F$  (depression-dominant, E2 type) and  $D \approx F$  (pseudolinear, E3 type) (**Fig. 4a**; **Table 1**). The patterns of excitatory postsynaptic potentials (EPSPs) during the train stimulation were also visually different (**Supplementary Fig. 3** online). These three clusters of synaptic dynamics were also found for GABAergic synaptic connections<sup>23</sup>. All 26 of the modeled visual cortex connections, even those with some degree of facilitation, fell into the E2 class.

The E1 and E2 connections each contained subdivisions distinguished by high (type a) and low (type b) values of *U* and the inverse for *A* (**Fig. 4b**). The inverse relationship between *U* and *A* indicates that the low probability synaptic connections were in fact stronger than the average connections and that the high probability synapses were weaker synapses. The E3 connections also contained subdivisions distinguished by high (type a) and low (type b) values of *U*. But these subtypes differed from the E1 and E2 subtypes mainly in terms of either low (type a) or high (type b) *DF* value. *A* values also covaried with *U* in these subtypes, indicating that low probability connections contained weaker synapses and high probability connections contained stronger synapses (**Fig. 4b**).

The average *DFUA* values for the three types further illustrate that it is the *DF* ratios that primarily distinguish the synapses (**Table 1**). We observed three primary trends in the *DF* relationship (**Fig. 4c**): one in which *D* values ranged to above 1 s while *F* values were at or close to zero (vertical); one in which *F* values ranged to above 1 s while *D* values remained low (horizontal); and one in which both *D* and *F* values increased (oblique). To test the statistical reliability of the data falling into three clusters, we used bootstrap resampling of KMEANS clustering (where  $K = 3$ , based on the QTC findings

connections required low values of *F* (20–50 ms) for an optimal fit. Extracting the *DFUA* parameters for all the connections showed that the mean *F* at mPFC synaptic connections was about 20 times longer than that at visual cortex connections (296 ms versus 14 ms; **Fig. 3** and **Table 1**). A comparison of the probability density function for *F* also showed that the distribution was at least bimodal in the mPFC, compared with a unimodal distribution in visual cortex. The mean *D* and *A* parameters were not statistically different in the two cortical regions ( $P = 0.184$  and  $P = 0.584$ ), but the probability density function for *D* showed a trimodal distribution in which the median was statistically different in a Kolmogorov-Smirnov test (**Fig. 3**;  $P = 0.0374$ ). These results are consistent with the dominating synaptic depression found in the visual cortex of adult rats and cats<sup>13–18</sup>.

We also screened synaptic connections in a number of neocortical regions in the mPFC ( $n = 34$ ), visual cortex ( $n = 24$ ), auditory cortex ( $n = 20$ ) and somatosensory cortex ( $n = 31$ ) of juvenile rats. These results showed a notable difference in the *F* in the mPFC as compared with the other neocortical regions ( $P = 3.2 \times 10^{-6}$ , analysis of variance (ANOVA), **Supplementary Fig. 2** online). We also found these facilitating synapses in the juvenile mouse mPFC (J. Couey & H. Markram, unpublished data), suggesting that this could be a general feature of mammalian mPFC. We also recorded powerful facilitating synapses in the adult rat mPFC (1- to 2-months-old;  $n = 3$ ; data not shown), indicating that this is not merely a transient expression of facilitation in certain species.

Synaptic depression has been extensively reported for interpyramidal connections in all layers and in particular for layer 5 pyramidal synapses in the juvenile and adult rat somatosensory, motor and visual cortices<sup>13–15,17–20</sup> and in cats<sup>14,17,21</sup>. However, facilitation has been observed for some synapses formed between layer 5 pyramidal cells in the adult sensorimotor cortex<sup>12</sup> and between some subtypes of layer 6 pyramidal cells in the adult rat and cat neocortex<sup>22</sup>. We also

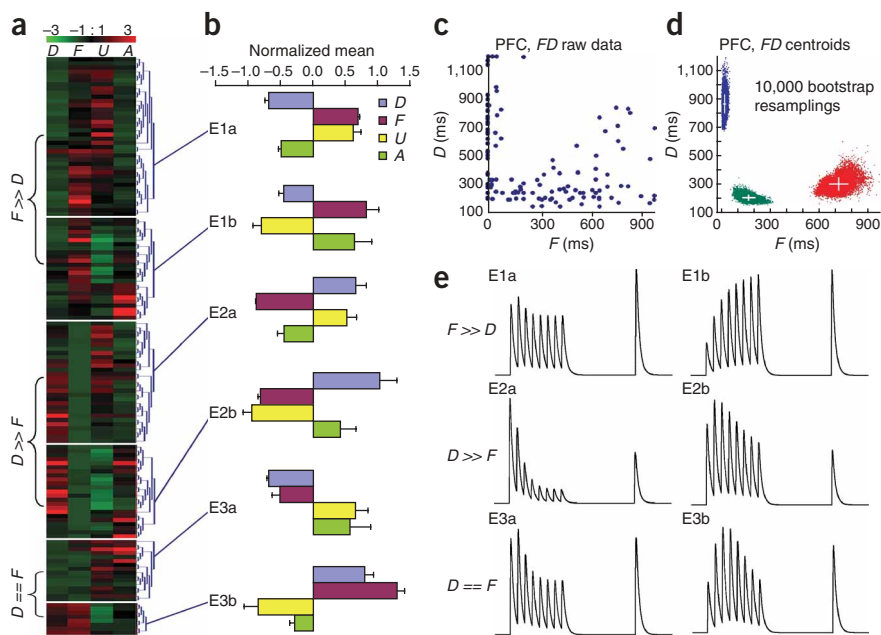


**Figure 4** Excitatory synaptic subtypes in the mPFC. **(a)** Quality threshold clustering (QTC) of  $DFUA$  values for all modeled connections. Pseudocolor scale represents  $z$ -normalized values. **(b)** Bar graphs summarize normalized means ( $\pm$  s.e.m.) of the six subclusters in **a**. E1 groups, two clusters with  $F > > D$ ; E2 groups, two clusters with  $D > > F$ ; and E3 groups, two clusters with  $F$  similar to  $D$ . E1 and E2 groups each contained two subclusters with high (E1a, E2a) and low (E1b, E2b) values of  $U$  and the converse for the absolute synaptic strength,  $A$ . The E3 group also contained two clusters with low (E3a) and high (E3b)  $D$  and  $F$ . The values of  $U$  and  $A$  were also flipped, but unlike the E1 and E2 connections, they covaried. **(c)**  $F$  versus  $D$  plot based on all 139 modeled mPFC connections. Three  $DF$  regions were apparent here (and from **a**): one with higher  $D$  values and lower  $F$  values (vertical); one with higher  $F$  values and lower  $D$  values (horizontal); and one with both  $D$  and  $F$  values increased (oblique). **(d)** KMEANS clustering assuming three classes of  $DF$  relationships. The KMEANS algorithm computed the maximal possible separation of the three  $DF$  ratios using 10,000 bootstrap resamplings. The three centroids found by KMEANS are entirely separate. **(e)** Model responses generated by using the characteristic  $DFU$  parameters in each QTC derived cluster from **a** and **b**.

above) to find the maximal possible separation of the three  $DF$  relationships (10,000 bootstrap resamplings; **Supplementary Methods**). The strong separation of the centroids was highly significant (**Fig. 4d**;  $P = 1 \times 10^{-9}$  by ANOVA; see also linear discriminant analysis in **Supplementary Methods**), indicating a significant trend for the parameters to cluster in three configurations. Note that this analysis does not mean that there is no overlap among individual synaptic populations; rather, it demonstrates the significance of the tendency for the parameters to cluster. It therefore illustrates the idealization or means of the different parameter configurations. Model responses using the characteristic  $DFU$  parameters in each class illustrate the widely different forms of synaptic dynamics observed in the mPFC pyramidal circuit (**Fig. 4e**).

### Pronounced synaptic augmentation and PTP

Potentiation in synaptic responses lasting up to 10 s, known as synaptic augmentation<sup>24</sup>, is enhanced in the rat mPFC (ref. 6). To investigate the synaptic basis of this augmentation in the layer 5 pyramidal network of the mPFC, we recorded single action potential-evoked responses (0.5 Hz) before and after a tetanic train of 15 presynaptic action potentials at 50 Hz. We observed substantial synaptic augmentation (nearly 50%) among E1 connections, with a single-decay time constant of 4.2 s (**Fig. 5a,b**); there was no statistical evidence to support more than a single exponential fit. This is consistent with the previous report,

which showed that synaptic augmentation is enhanced in the mPFC compared with the visual cortex<sup>6</sup>; moreover, our result extends this finding by showing that this synaptic augmentation occurs mainly at the facilitating E1 and E3 synapses (**Fig. 5a,b**; also see below for the pyramidal subnetwork supporting synaptic augmentation). We also found that E1 connections showed not only synaptic augmentation, but also PTP, a post-tetanic potentiation that lasts longer than 30 s and up to a few minutes, as described previously<sup>24</sup>. Our recording time frame was limited to 100 s after the tetanus; the synaptic responses of the E1 connections remained elevated by  $14.9 \pm 0.5\%$  during the 30- to 100-s period (difference between E1 and E2 = 0.119 mV;  $P = 0.0013$ , two-tailed  $t$ -test). During this time window, E2 and E3 connections had essentially recovered to baseline (**Fig. 5c**). The E2 connections in the mPFC did not show PTP but did show a small amount of synaptic augmentation (**Fig. 5a,b**). E2 connections in the visual cortex showed similar changes as E2 connections in mPFC ( $n = 12$ ; data not shown for synaptic augmentation; **Fig. 5c** for PTP). E3 connections in mPFC showed stronger synaptic augmentation than the E2 connections ( $P = 0.05$ ), but this seemed weaker than that of the E1 connections; also, the E3 connections did not show PTP (**Fig. 5c**, **Supplementary Table 2** online). The expression of synaptic augmentation therefore seems to correlate with the strength of synaptic facilitation, whereas PTP is found only in the E1 synapses. The relationship between synaptic augmentation and/or PTP

and the synapse types also provided independent confirmation of these major types of excitatory synapses in the mPFC.

### Hyper-reciprocity using facilitating synapses

The averaged probability of pyramidal cells being connected was only marginally higher in the mPFC than in the visual cortex (12% versus 10%), but the probability of forming reciprocal connections was more than double in the mPFC compared with visual cortex (**Fig. 6a**, 47% versus 18%;  $P = 0.0016$ ,  $\chi^2$  test; **Supplementary Tables 1 and 2**), suggesting a new form of hyper-reciprocity compared with other neocortical regions<sup>15,25</sup>. Among all reciprocal pairs ( $n = 34$ ), 82% involved E1 connections (44% used E1 in both directions). Also, 68% of E1 and 63% of E3 synapses were involved in the reciprocal connections, significantly greater than the 23% involvement of E2 synapses (E1 versus E2:  $P = 1.4 \times 10^{-6}$ ; E3 versus E2:  $P = 0.0008$ ;  $\chi^2$  test). These data suggest that not only does the pyramidal network in the mPFC contain synapses with powerful facilitation, pronounced synaptic augmentation and PTP, but these facilitating synapses are also primarily deployed in a new form of hyper-reciprocity.

### Differential synaptic transmission

A given presynaptic neuron can form depressing synapses onto one neuron and facilitating synapses onto another<sup>8</sup>, and the type of synapse is directly correlated with the anatomy and physiology of the type of

pre- and postsynaptic neurons<sup>11,23,26</sup>. This has been shown only for fundamentally different targets, such as interneurons versus pyramidal cells, and not for targets within the same morphological class, such as between pyramidal cells. The different types of synapses we found in the mPFC may therefore suggest that the pyramidal cells in the mPFC are sufficiently diverse to demonstrate differential expression of synaptic properties. At least three subpopulations of pyramidal cells would then be predicted from the three types of excitatory synapses.

To better understand the differential transmission within and between these putative subpopulations of pyramidal cells in the mPFC, we further examined the types of synapses found in divergent, convergent and reciprocal connections. Most divergent connections were formed by the same type of connection, ( $n = 7$  of 11; E1: 2 of 7; E2: 5 of 7); however, we also observed connections with different types (E1–E2: 2 of 11; E1–E3: 1 of 11; E2–E3: 1 of 11; **Fig. 6b**; **Supplementary Table 1**). Most of the reciprocal connections were also formed with the same type of synapse in both directions (**Fig. 6a**;  $n = 20$  of 34 pairs, or 59%; E1: 44%; E2: 9%; E3: 6%), and the remainder were formed with different types of synapses ( $n = 14$  of 34, or 41%; E1–E3: 26%; E1–E2: 9%; E2–E3: 6%). Pyramidal cells also received different types of synapses (E1–E2: 2 of 5; **Fig. 6c**), but mostly they also received the same types of synapses (E1: 3 of 5) from other pyramidal cells in the convergent connections (**Supplementary Table 1**). This evidence indicated that pyramidal cells innervate pyramidal cells more frequently within, rather than across, their subpopulations in the mPFC and that the determination of the synaptic dynamics is not solely dependent on the targets but rather on pre- and postsynaptic combinations. Such a combinatorial synaptic determination also exists for GABAergic synapses<sup>23</sup>.

**Table 1** Types and subtypes of excitatory connections in mPFC and VC

	<i>D</i> (ms)	<i>F</i> (ms)	<i>U</i>	<i>A</i>	<i>D/F</i>	<i>F/D</i>
PFC-E1 ( $n = 63$ )	194 ± 18	507 ± 37	0.28 ± 0.02	3.32 ± 0.40	0.38	2.61
E1a ( $n = 38$ )	163 ± 20	482 ± 47	0.35 ± 0.02	1.95 ± 0.15	0.34	2.96
E1b ( $n = 25$ )	242 ± 28	563 ± 60	0.17 ± 0.02	5.35 ± 0.82	0.43	2.33
PFC-E2 ( $n = 52$ )	671 ± 17	17 ± 5	0.25 ± 0.02	3.24 ± 0.25	39.47	0.03
E2a ( $n = 29$ )	615 ± 56	8 ± 4	0.34 ± 0.02	2.07 ± 0.30	76.88	0.01
E2b ( $n = 23$ )	741 ± 89	29 ± 11	0.15 ± 0.02	4.73 ± 0.69	25.55	0.04
PFC-E3 ( $n = 24$ )	329 ± 53	326 ± 66	0.29 ± 0.03	4.30 ± 0.69	1.01	0.99
E3a ( $n = 16$ )	164 ± 12	130 ± 43	0.35 ± 0.02	5.16 ± 0.98	1.26	0.79
E2b ( $n = 8$ )	661 ± 48	718 ± 36	0.16 ± 0.03	2.58 ± 0.24	0.92	1.09
VC-E2 ( $n = 26$ )	463 ± 84	6 ± 4	0.21 ± 0.03	3.69 ± 0.64	77.17	0.01

PFC classification was derived from the QTC analysis; VC EPSP patterns all correspond to PFC E2-like physiology.

### Subnetworks of pyramidal cells

The pyramidal cells in the PFC are perhaps the most morphologically complex in the neocortex<sup>27</sup>, but subtypes have not been defined. We found two major subtypes of pyramidal cells in layer 5 of the mPFC: those bifurcating very early (most in layer 5, some on the border of layers 4 and 5, and a few in layer 4) to give rise to dual apical dendrites, referred to as complex pyramidal cells (cPC; **Fig. 6d**); and those that are similar to typical pyramidal cells elsewhere in neocortex, with a single apical dendrite ascending and bifurcating in superficial layers to form the tuft dendrites, referred to as simple pyramidal cells (sPC; **Fig. 6e**). Three-dimensional (3D) computer reconstructions showed that cPCs, compared with sPCs, have almost twice the total apical dendritic length and significantly more extensive and frequently branching basal dendrites ( $P < 0.05$ , two-tailed *t*-test; **Supplementary Table 3** online). The cPC is the most common form of pyramidal cell in the mPFC (89%,  $n = 101$ ), whereas the sPC is the most common pyramidal cell in the visual cortex (87%,  $n = 24$ ; **Supplementary Table 1**). Thus, similar to the case for facilitating

**Figure 5** Synaptic augmentation and post-tetanic potentiation (PTP) in different types of excitatory connections in the mPFC. **(a)** Inductions of synaptic augmentation in single synaptic connections. We recorded single action potential-evoked testing responses (0.5 Hz) 20 s before and 100 s after a tetanus of 15 presynaptic action potentials at 50 Hz, repeated 4 times at intervals of 2 min. Each EPSP was averaged from 12 single EPSPs by using a moving window. Note that every second trace is shown, due to the limited space. **(b)** Synaptic augmentation in E1- and E2-type connections in the mPFC. Testing EPSP amplitudes (± s.e.m.) were averaged from E1 and E2 groups of connections; values are normalized to the mean of 40 traces before the tetanus. The synaptic augmentation for E1 synapses was much greater than that for E2 (initial increments: 44.6% for E1 versus 10% for E2;  $P = 0.0009$ , two-tailed *t*-test). Inset, single-exponential time constant, fit to the recovery of synaptic augmentation in E1 synapses. **(c)** PTP in different types of connections of the mPFC and visual cortex. During the 30- to 100-s period after the tetanus, the averaged EPSP amplitude increment of E1 connections in the PFC was 14.9 ± 0.5% (or 33.4% of initial synaptic augmentation responses), whereas E2 and E3 connections in the PFC and E2 connections in the visual cortex had virtually recovered (PFC: E2 = 2.8 ± 0.5%, E3 = 0.3 ± 0.9%; visual cortex: E2 = 1.6 ± 0.6%;  $P = 0.002$  for PFC E1 versus E2 and E3, and for PFC E1 versus visual cortex E2, ANOVA).

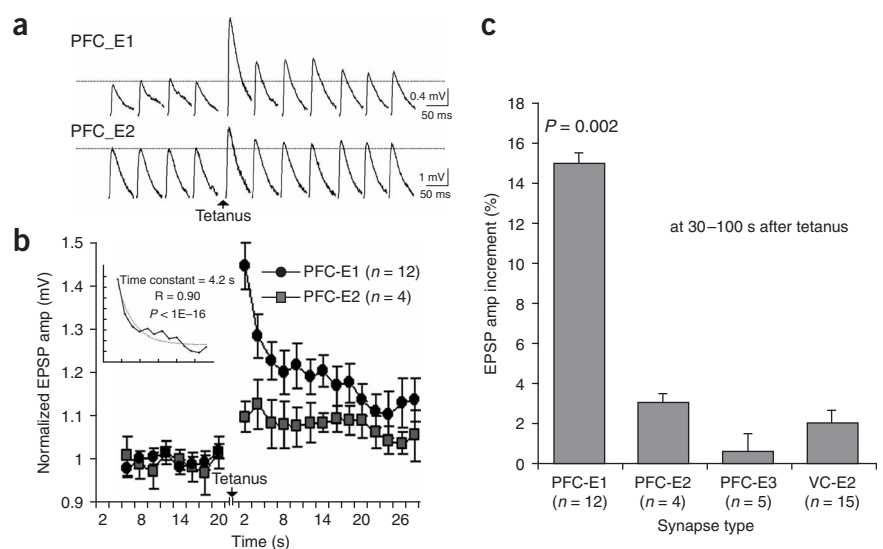
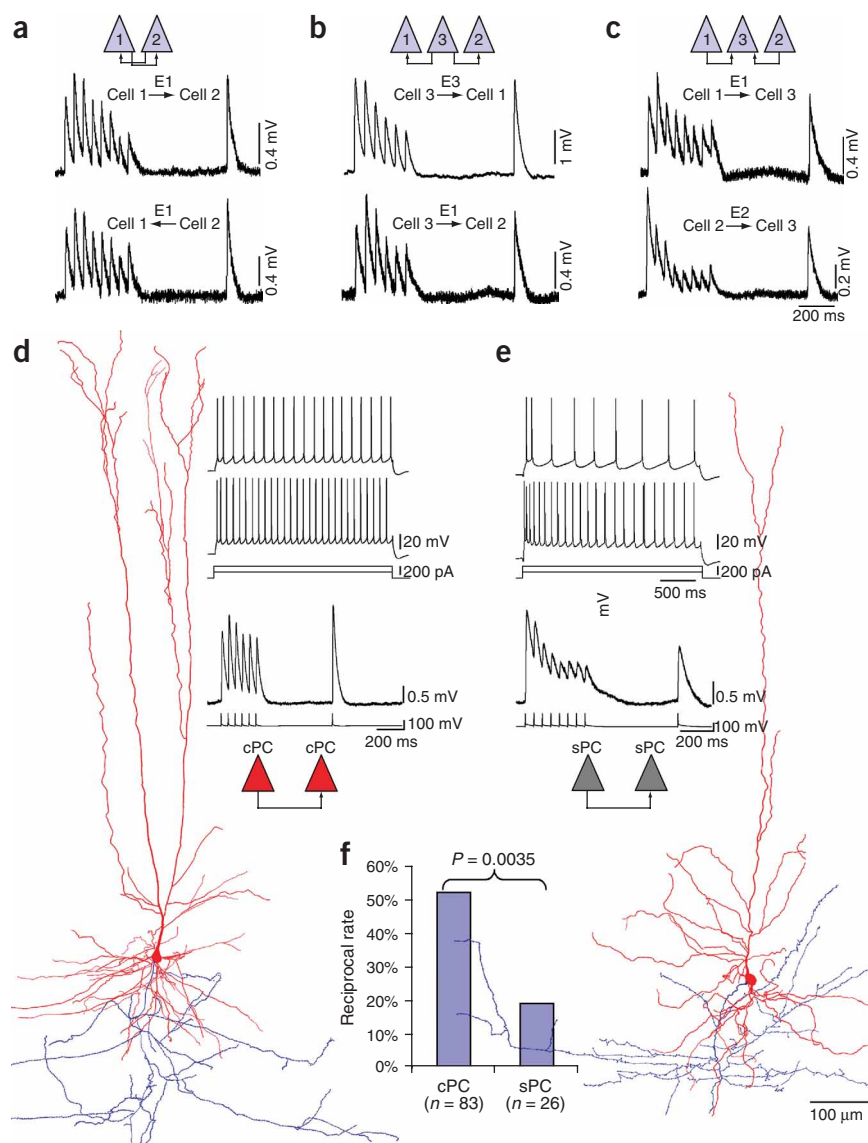


**Figure 6** Functional and structural architecture of the layer 5 pyramidal network in the mPFC. (a) The same type of synaptic connection (E1) is used in a reciprocal connection between two cPCs. (b) Different synaptic types involved in divergent connections. (c) Different synaptic types involved in convergent connections. (d) Reconstructed cPC (red, soma and dendrites; blue, axon). Note that the apical dendrite bifurcates immediately in layer 5 to give rise to dual apicals. cPCs mainly showed nonaccommodating discharge behavior and sustained excitation (action potential traces in upper panel), and commonly received E1- and E3-type connections from other cPCs (postsynaptic trace in lower panel). (e) Reconstructed sPC. Note that only one apical dendrite ascends and bifurcates in layer 2/3 to form the tuft dendrites. sPCs mainly showed accommodating discharge behavior (action potential traces in upper panel) and often received E2-type synaptic connections (postsynaptic trace in lower panel) from other sPCs. (f) Hyper-reciprocity of cPCs as compared with sPCs ( $P = 0.0035$ ,  $\chi^2$  test). cPCs are much more likely to be reciprocally connected than sPCs.



synapses, this cellular feature may not be unique to the mPFC, but it is certainly a major feature.

Electrophysiologically, pyramidal cells are typically classified as accommodating or nonaccommodating, according to their firing in response to the injection of depolarizing step currents. The degree of adaptation, measured by the ratio of first to last interspike intervals near threshold depolarization, differed significantly for these two types of cell (accommodating:  $0.45 \pm 0.15$ ,  $n = 75$ ; nonaccommodating:  $0.98 \pm 0.12$ ,  $n = 88$ ;  $P = 5.4 \times 10^{-31}$ , two-tailed  $t$ -test **Fig. 6d,e**). The firing of the sPCs was accommodating and that of the cPCs was predominantly nonaccommodating (**Supplementary Table 4** online,  $P < 0.05$ ,  $\chi^2$  test), consistent with previous studies<sup>27</sup>.

The facilitating synapses, E1 and E3, primarily interconnected cPCs (52 of 54 pairs; **Supplementary Table 1**), whereas the E2 synapses mainly connected sPCs with one another and with cPCs (**Supplementary Table 1**). Consistently, E1 and E3 synapses primarily interconnected the nonaccommodating pyramidal cells, whereas E2 synapses predominantly interconnected the typical accommodating pyramidal cells (**Fig. 6d,e**; **Supplementary Tables 1** and **2**;  $P < 0.05$ ,  $\chi^2$  test). In addition, cPCs had a much higher rate of reciprocal connections than did sPCs in the mPFC (**Fig. 6f**). Also, 83% of reciprocal connections between cPCs were made by the E1 and E3 synapses. In contrast, reciprocal connections among sPCs were made most often with E2 synapses, as was also the case in the visual cortex and in other cortices<sup>15,25,28</sup>. Furthermore, the number of putative synapses connecting cPCs was unusually high (12, 8 and 7 contacts per connection in three reconstructions, compared with the expected  $\sim 5$  contacts per connection in sensory areas; example in **Fig. 1a**). The significant correlations between E types and the neuronal morphology,

electrophysiology, reciprocity and network properties provide further independent confirmations of the synaptic clustering.

## DISCUSSION

This study shows the cellular features (elaborate morphologies and nonaccommodating spiking), synaptic properties (powerful facilitation, pronounced synaptic augmentation and PTP) and connectivity properties (high reciprocal rate, high number of putative synaptic contacts) of a complex and highly heterogeneous microcircuit of pyramidal cells in the mPFC. These could favor enhanced recurrent excitation in the microcircuit, which may be important for persistent activity.

### Recurrent excitation in the PFC

The PFC is a neocortical region that is highly interconnected with other neocortical and subcortical regions, as evidenced by extremely elaborate divergent axonal projections from the layer 5 pyramids to other areas and by the elaborate dendritic arborization in the neocortex for receiving input from many brain regions<sup>4,5,29-31</sup>. This high level of interconnectivity with the rest of the neocortex could serve to support long-range reverberant activity, which may be an important part of

initiating and maintaining persistent activity in the PFC. In addition to these extrinsic features, there are a number of possible intrinsic features that could allow the PFC to be activated and to remain active in a 'holding pattern' on its own, without any further input support. This is partly suggested by the behavioral evidence that animals can maintain persistent neuronal activity in the PFC even when the stimulus signal is switched off, but more convincingly by the fact that the persistent activity remains while the animal also handles distracting stimuli that may be competing for resources<sup>1,2</sup>. A number of factors could be important in generating the persistent activity state in the prefrontal cortex, but to determine which properties are actually available in this cortical region, it is essential to understand the specific cellular, synaptic and network properties of the layer 5 pyramidal network in the PFC that forms the core of the recurrent excitatory circuitry.

### Pyramidal subpopulations

The morphological complexity of neurons increases from primary sensory and motor areas through association areas, reaching its most elaborate forms in the PFC (see review ref. 27). We found a large number of pyramidal cells with early apical bifurcations that form dual apical dendrites. Even visually, this type of cell is notably different from the typical pyramidal cell, and a detailed morphometric analysis showed that the total apical dendritic lengths of these cPCs is basically double that of the sPCs and that their basal dendritic clusters are substantially wider and denser and have more dendritic branches. Apical dendrites enable pyramidal cells to receive input from different layers, allowing cross-layer integration, and the early bifurcation provides a dual set of tuft dendrites, which receive multimodal input from the neocortex as well as nonspecific and associative input from the thalamus. The tuft dendrites in layer 1 contain a number of voltage-activated channels, such as Ca<sup>2+</sup> channels, that amplify input signals by generating Ca<sup>2+</sup> spikes<sup>32–34</sup>, and the dual apical structure may therefore allow a broader and more efficient integration of information in layer 1. The tuft dendrites also contain the ion channels carrying large I<sub>h</sub> currents (the Na<sup>+</sup> and K<sup>+</sup> currents activated by hyperpolarization of membrane potentials)<sup>35,36</sup>, which seem to regulate up states: blocking I<sub>h</sub> greatly enhances up states, prolonging their duration and increasing their frequency (D.A. McCormick, personal communication). cPCs also show tonic nonaccommodating behavior, which might help these cells to sustain their activity at high rates whenever it is needed. Therefore, the morphology and electrical properties of these cPCs with dual apical dendrites and wide and dense basal dendrites may provide the specializations essential for supporting persistent activity in the PFC.

### Hyper-reciprocity in the mPFC

The elaborate morphology of the cPCs could also support more local recurrent synapses to form a stronger recurrent circuit. The axodendritic contacts are random for layer 5 pyramidal cells<sup>37</sup>, and it is likely that more elaborate local dendritic and axonal arborizations would increase the number of axodendritic contact sites between any two pyramidal cells. Indeed, we found an unusually high number of putative synapses between cPCs. The microcircuit in the mPFC is therefore potentially a stronger recurrent circuit than that in most neocortical regions.

The averaged probability of pyramidal cells being connected in the mPFC was about the same for layer 5 as in other sensory areas (typically 10–15%), but the probability of forming reciprocal connections was remarkably high in general, especially between the cPCs in the mPFC. Hyper-reciprocity (as compared with the average connection probability) was originally reported in the rat somatosensory cortex<sup>19</sup> but the

rates were mostly lower than 30% (refs. 15,19,21,25), which is similar for the sPCs in the mPFC.

Hyper-reciprocity could contribute toward the stability of recurrent excitation by forming strong local attractors. Such reciprocity of pyramidal cells could also act to synchronize and isolate information processing within a subpopulation, allowing functionally separate subnetworks to coexist side by side. The pyramidal cells with the highest reciprocal rates are the cPCs interconnected with E1 synapses and those with the lowest reciprocal rates are the sPCs interconnected with E2 synapses (E1 > E3 > E2). The unidirectional nature and low rate of reciprocal connections between different pyramidal cells and with different synapses could shape the integration across subnetworks. The high reciprocity of the layer 5 cPCs therefore seems to contribute to the battery of microcircuit properties that could support a more robust form of persistent activity in the PFC.

### Synaptic facilitation in the mPFC

A recurrent network enters into a state of reverberant excitation when the recurrent synapses are sufficiently strong to sustain the excitation<sup>38,39</sup>. Synaptic facilitation could, in principle, allow the strength of the synapses to increase during activity above this recurrent excitation threshold to cause reverberant activity<sup>5,40</sup>. The current study showed notable facilitation for the majority of synapses formed between pyramidal cells in the mPFC; this differs from the predominant synaptic depression typically found in the primary sensory cortices of young<sup>12,13,18–20</sup> and adult animals<sup>13,14,16,21</sup>. Furthermore, the facilitating synapses in the mPFC have high release probabilities that contrast with the low release probabilities of the facilitating synapses in other cortical areas<sup>8,10–12</sup>. This high probability of release could mask the functional facilitation in the mPFC, which could have important consequences for setting the optimal frequency for maximal transmission. The optimal frequencies for peak amplitudes can be computed using the *DFU* values and is in the low Hz range for these facilitating synapses<sup>8,9</sup>. Dopamine, an important neuromodulator involved in attention and working memory, lowers *p* considerably at these synapses<sup>41</sup>, which could shift the peak frequency upward to above 40 Hz. This synaptic design may therefore allow such neuromodulatory systems to control the dynamic range of frequency preferences and hence the conditions under which facilitation has a role in the mPFC. Synaptic facilitation is, however, not unique to the mPFC and is therefore likely to be just one of the battery of features that characterize the mPFC and collectively support the special forms of activity in this region.

### Synaptic augmentation and PTP in the mPFC

Pronounced synaptic augmentation and PTP are also common phenomena found between cPCs in the mPFC. Not only were these properties uncommon in the primary visual cortex of the ferrets, but they were also not significantly expressed in the E2 synapses even within the mPFC. E3 synapses did show synaptic augmentation but no significant PTP whereas E1 synapses showed both synaptic augmentation and PTP, suggesting that pronounced synaptic augmentation is coexpressed at moderately facilitating synapses and PTP is found only at synapses with pronounced facilitation in the mPFC. Facilitation lasting hundreds of milliseconds, synaptic augmentation lasting up to 10 s, and PTP lasting up to minutes may be important to sustain the activity during short-term memories like those involved in a working memory task<sup>42,43</sup>. Indeed, a simple neuronal model shows that synaptic augmentation alone can enable the weak recurrent connections to support persistent activity following a transient input<sup>6</sup>.

### Implications for persistent activity

This study shows that the mPFC displays many cellular, synaptic and network specializations that could act to amplify, orchestrate and maintain the recurrent network activity and hence support persistent activity. It will, however, require a detailed model of the microcircuitry to show precisely how each of these parameters contributes to the special properties of the mPFC. The different frequency preferences for these subnetworks could allow new forms of reverberation within and between subnetworks. Given that neuromodulators can change  $p$  significantly, it is possible that they have a crucial role in shaping which holding patterns should be maintained and for how long. Input to the E2 subnetwork could, for example, initiate recurrent network activity, which may be transferred to the E3 subnetwork where facilitation may filter the transferred input signals while synaptic augmentation and the higher reciprocity may provide additional robustness. If the recurrent network activity survives for long enough or is salient enough, the E1 subnetwork may also be recruited into the active state where the high reciprocity, synaptic augmentation, PTP and the elaborate morphologies of the cPCs as well as their nonaccommodating discharges could sustain and protect the holding pattern of activity in the face of distractors. A prediction would then be that input to the E1 subnetwork could terminate this active state. This could perhaps be achieved by strong excitation to the tuft dendrites of the cPCs, which can evoke  $\text{Ca}^{2+}$  spikes in the tufts of dual apical dendrites<sup>44</sup> resulting in a high frequency burst of the cPCs, thereby depressing synapses to below recurrent excitation thresholds. It is interesting that *in vivo* experiments first indicated the existence of subnetworks in the PFC (ref. 3).

### METHODS

**Slice preparation.** Slices were prepared from young ferrets (1.5- to 3-months-old) following published protocol<sup>41</sup>. The artificial cerebrospinal fluid (ACSF) solution contained 125 mM NaCl, 2.5 mM KCl, 25 mM glucose, 25 mM  $\text{NaHCO}_3$ , 1.25 mM  $\text{NaH}_2\text{PO}_4$ , 2 mM  $\text{CaCl}_2$  and 1 mM  $\text{MgCl}_2$ . Neurons in layer 5 were identified using infrared differential contrast videomicroscopy with an upright microscope (BX50WI, Olympus), according to the pyramidal shape of the soma and the thick primary apical dendrites typical of pyramidal cells. All experiments were carried out in accordance with the requirements of our institutional Animal Use and Care Committee.

**Electrophysiological recording.** We made somatic whole-cell recordings (pipette resistance 6–12 m $\Omega$ ) in which signals were amplified using Axoclamp-200B amplifiers (Axon Instruments). Recordings were sampled at intervals of 10–400  $\mu\text{s}$  and filtered at 3 kHz, 10 kHz or 30 kHz using the Igor program (Igor Wavemetrics), digitized by an ITC-18 interface (Instrutech) and stored on a hard drive (Macintosh G4) for offline analysis. Voltages were recorded with pipettes containing 100 mM potassium gluconate, 20 mM KCl, 4 mM ATP-Mg, 10 mM phosphocreatine, 0.3 mM GTP, 10 mM HEPES buffer (pH 7.3) and 0.4% biocytin (Sigma). Neurons were filled with biocytin by diffusion during recordings. The basal transmission of a connection was recorded with a train of 6–8 EPSPs, mostly at 20 Hz, and a recovery test response after a 500-ms delay. We induced synaptic augmentation by giving a 15-pulse stimulus at 50 Hz (tetanus). Single test responses (0.5 Hz) were recorded for 20 s before and 100 s after the tetanus. The whole procedure was repeated 4 times with a 2-min interval. Membrane potentials were routinely current-clamped at  $-70$  mV.

**Histological procedures and 3D computer reconstruction.** After recording, the slices were fixed for at least 24 h in cold 0.1 M phosphate buffer (pH 7.4) containing 2% paraformaldehyde and 1% glutaraldehyde. Thereafter, the slices were rinsed and then transferred into phosphate-buffered 3%  $\text{H}_2\text{O}_2$  to block endogenous peroxidases. After rinsing in phosphate buffer, slices were incubated overnight at 4 °C in avidin-biotinylated horseradish peroxidase (ABC-Elite, Vector Labs; 2% A, 2% B and 1% Triton X-100). Subsequently, sections were rinsed again in phosphate buffer and developed with diaminobenzidine under visual control using a bright-field microscope (Zeiss

Axioskop) until all processes of the cells were clearly visible. The reaction was finally stopped by transferring the sections into phosphate buffer. After rinsing in phosphate buffer, slices were mounted in aqueous mounting medium.

We reconstructed 3D neuron models using the NeuroLucida system (MicroBrightField) and a bright-field light microscope (Olympus, BX51). Subsequently, we analyzed the reconstructed neurons and their connections quantitatively using NeuroExplorer (MicroBrightField). Putative synapses were identified according to the following criteria: (i) only contacts forming by axonal swellings (boutons) were considered; (ii) the same plane of focus was used (microscope lens with 60 $\times$  magnification, numerical aperture = 0.9; resolution along the z-axis = 0.37  $\mu\text{m}$ ), which requires the bouton and the somatic, dendritic or axonal membranes to be within  $<0.5$   $\mu\text{m}$  of each other; (iii) if the dendrite was thick ( $>2$   $\mu\text{m}$ ) with many spines, then a greater distance between the bouton and the dendrite was allowed, providing that the axon bent toward or ran parallel with the dendrite.

**Nomenclature for the classification of excitatory synaptic connections.** Our rationale for naming excitatory synaptic connections as E1 (facilitation-dominant), E2 (depression-dominant) and E3 (facilitation- and depression-balanced) was that (i) these E types as excitatory synaptic classes correspond to previously reported inhibitory synaptic classes<sup>23</sup> (F1, facilitation-dominant; F2, depression-dominant; and F3, facilitation- and depression-balanced); and (ii) E1 as excitatory facilitating type and E2 as excitatory depressing type have been published for connections of pyramidal cells innervating interneurons<sup>26</sup>.

**Statistical analysis.** We used Student *t*-tests, ANOVAs and  $\chi^2$  tests for statistical comparisons of two groups, multiple groups, and rates, respectively. We used kernel smoothing to facilitate visual comparison of parameter distributions among cortical areas. Synaptic clusters were generated using QTC. Because QTC consistently found three major clusters, we applied KMEANS with  $K = 3$  using 10,000 bootstrap replications to validate the reliability of the separation of the cluster means. Because cluster analysis does not use a *priori* knowledge of group membership, we used discriminant analysis to test the consistency of clustering on the basis of the DFUA measurements (**Supplementary Methods**).

*Note: Supplementary information is available on the Nature Neuroscience website.*

### ACKNOWLEDGMENTS

This paper is dedicated to Patricia S. Goldman-Rakic, who wholeheartedly supported and supervised this study before she passed away suddenly on July 31 2003. She will always be an inspiration for our work. We are grateful to D.A. McCormick, T. Koos and W.J. Gao for comments on the experimental design; O. Melamed for testing mathematical synaptic modeling; and M. Pappy and A. Begovic for technical assistance. We also thank M. Tsodyks for performing preliminary network modeling studies to better understand the potential functions of facilitation and PTP in recurrent excitation and for his comments on the paper. This work was supported by the National Institute of Mental Health (grant RO1), the Natalie V. Zucker Award, the Charlton Research grants to Tufts University School of Medicine and, in part, by the National Alliance for Autism Research.

### AUTHOR CONTRIBUTIONS

Y.W. designed the experiments and did most of the experiments. H.M. did the modeling for the synaptic connections. P.H.G. did the clustering analysis for the different classes of synaptic connections. T.K.B. did some of the experiments. J.M. did 3D computer reconstruction of the neurons and connections. P.S.G.-R. supervised this study before she passed away. Y.W. and H.M. wrote the manuscript.

### COMPETING INTERESTS STATEMENT

The authors declare that they have no competing financial interests.

Published online at <http://www.nature.com/natureneuroscience>  
Reprints and permissions information is available online at <http://npg.nature.com/reprintsandpermissions/>

1. Goldman-Rakic, P.S. Cellular basis of working memory. *Neuron* **14**, 477–485 (1995).
2. Miller, E.K., Erickson, C.A. & Desimone, R. Neural mechanisms of visual working memory in prefrontal cortex of the macaque. *J. Neurosci.* **16**, 5154–5167 (1996).
3. Goldman-Rakic, P.S. Architecture of the prefrontal cortex and the central executive. *Ann. NY Acad. Sci.* **769**, 71–83 (1995).



4. Wang, X.J. Synaptic reverberation underlying mnemonic persistent activity. *Trends Neurosci.* **24**, 455–463 (2001).
5. Durstewitz, D., Seamans, J.K. & Sejnowski, T.J. Neurocomputational models of working memory. *Nat. Neurosci.* **3**, 1184–1191 (2000).
6. Hempel, C.M., Hartman, K.H., Wang, X.J., Turrigiano, G.G. & Nelson, S.B. Multiple forms of short-term plasticity at excitatory synapses in rat medial prefrontal cortex. *J. Neurophysiol.* **83**, 3031–3041 (2000).
7. Thomson, A.M., Deuchars, J. & West, D.C. Single axon excitatory postsynaptic potentials in neocortical interneurons exhibit pronounced paired pulse facilitation. *Neuroscience* **54**, 347–360 (1993).
8. Markram, H., Wang, Y. & Tsodyks, M. Differential signaling via the same axon of neocortical pyramidal neurons. *Proc. Natl. Acad. Sci. USA* **95**, 5323–5328 (1998).
9. Tsodyks, M.V. & Markram, H. The neural code between neocortical pyramidal neurons depends on neurotransmitter release probability. *Proc. Natl. Acad. Sci. USA* **94**, 719–723 (1997).
10. Thomson, A.M. Facilitation, augmentation and potentiation at central synapses. *Trends Neurosci.* **23**, 305–312 (2000).
11. Reyes, A. *et al.* Target-cell-specific facilitation and depression in neocortical circuits. *Nat. Neurosci.* **1**, 279–285 (1998).
12. Reyes, A. & Sakmann, B. Developmental switch in the short-term modification of unitary EPSPs evoked in layer 2/3 and layer 5 pyramidal neurons of rat neocortex. *J. Neurosci.* **19**, 3827–3835 (1999).
13. Abbott, L.F., Varela, J.A., Sen, K. & Nelson, S.B. Synaptic depression and cortical gain control. *Science* **275**, 220–224 (1997).
14. Mercer, A. *et al.* Excitatory connections made by presynaptic cortico-cortical pyramidal cells in layer 6 of the neocortex. *Cereb. Cortex* **15**, 1485–1496 (2005).
15. Thomson, A.M., Deuchars, J. & West, D.C. Large, deep layer pyramid-pyramid single axon EPSPs in slices of rat motor cortex display paired pulse and frequency-dependent depression, mediated presynaptically and self-facilitation, mediated postsynaptically. *J. Neurophysiol.* **70**, 2354–2369 (1993).
16. Thomson, A.M. Activity-dependent properties of synaptic transmission at two classes of connections made by rat neocortical pyramidal axons in vitro. *J. Physiol. (Lond.)* **502**, 131–147 (1997).
17. Thomson, A.M., West, D.C., Wang, Y. & Bannister, A.P. Synaptic connections and small circuits involving excitatory and inhibitory neurons in layers 2–5 of adult rat and cat neocortex: triple intracellular recordings and biocytin labelling in vitro. *Cereb. Cortex* **12**, 936–953 (2002).
18. Varela, J.A. *et al.* A quantitative description of short-term plasticity at excitatory synapses in layer 2/3 of rat primary visual cortex. *J. Neurosci.* **17**, 7926–7940 (1997).
19. Markram, H., Lubke, J., Frotscher, M., Roth, A. & Sakmann, B. Physiology and anatomy of synaptic connections between thick tufted pyramidal neurones in the developing rat neocortex. *J. Physiol. (Lond.)* **500**, 409–440 (1997).
20. Galarreta, M. & Hestrin, S. Frequency-dependent synaptic depression and the balance of excitation and inhibition in the neocortex. *Nat. Neurosci.* **1**, 587–594 (1998).
21. Tarczy-Hornoch, K., Martin, K.A., Stratford, K.J. & Jack, J.J. Intracortical excitation of spiny neurons in layer 4 of cat striate cortex in vitro. *Cereb. Cortex* **9**, 833–843 (1999).
22. West, D.C., Mercer, A., Kirchhecker, S., Morris, O.T. & Thomson, A.M. Layer 6 corticothalamic pyramidal cells preferentially innervate interneurons and generate facilitating EPSPs. *Cereb. Cortex* **16**, 200–211.
23. Gupta, A., Wang, Y. & Markram, H. Organizing principles for a diversity of GABAergic interneurons and synapses in the neocortex. *Science* **287**, 273–278 (2000).
24. Zucker, R.S. & Regehr, W.G. Short-term synaptic plasticity. *Annu. Rev. Physiol.* **64**, 355–405 (2002).
25. Mason, A., Nicoll, A. & Stratford, K. Synaptic transmission between individual pyramidal neurons of the rat visual cortex in vitro. *J. Neurosci.* **11**, 72–84 (1991).
26. Markram, H. *et al.* Interneurons of the neocortical inhibitory system. *Nat. Rev. Neurosci.* **5**, 793–807 (2004).
27. Elston, G.N. Cortex, cognition and the cell: new insights into the pyramidal neuron and prefrontal function. *Cereb. Cortex* **13**, 1124–1138 (2003).
28. Markram, H. A network of tufted layer 5 pyramidal neurons. *Cereb. Cortex* **7**, 523–533 (1997).
29. Giguere, M. & Goldman-Rakic, P.S. Mediodorsal nucleus: areal, laminar, and tangential distribution of afferents and efferents in the frontal lobe of rhesus monkeys. *J. Comp. Neurol.* **277**, 195–213 (1988).
30. Cavada, C. & Goldman-Rakic, P.S. Posterior parietal cortex in rhesus monkey: II. Evidence for segregated corticocortical networks linking sensory and limbic areas with the frontal lobe. *J. Comp. Neurol.* **287**, 422–445 (1989).
31. Gabbott, P.L., Warner, T.A., Jays, P.R., Salway, P. & Busby, S.J. Prefrontal cortex in the rat: projections to subcortical autonomic, motor, and limbic centers. *J. Comp. Neurol.* **492**, 145–177 (2005).
32. Yuste, R., Gutnick, M.J., Saar, D., Delaney, K.R. & Tank, D.W. Ca<sup>2+</sup> accumulations in dendrites of neocortical pyramidal neurons: an apical band and evidence for two functional compartments. *Neuron* **13**, 23–43 (1994).
33. Larkum, M.E., Zhu, J.J. & Sakmann, B. A new cellular mechanism for coupling inputs arriving at different cortical layers. *Nature* **398**, 338–341 (1999).
34. Rhodes, P.A. & Llinas, R.R. Apical tuft input efficacy in layer 5 pyramidal cells from rat visual cortex. *J. Physiol. (Lond.)* **536**, 167–187 (2001).
35. Berger, T., Larkum, M.E. & Luscher, H.R. High I(h) channel density in the distal apical dendrite of layer V pyramidal cells increases bidirectional attenuation of EPSPs. *J. Neurophysiol.* **85**, 855–868 (2001).
36. Magee, J.C. Dendritic hyperpolarization-activated currents modify the integrative properties of hippocampal CA1 pyramidal neurons. *J. Neurosci.* **18**, 7613–7624 (1998).
37. Kalisman, N., Silberberg, G. & Markram, H. The neocortical microcircuit as a tabula rasa. *Proc. Natl. Acad. Sci. USA* **102**, 880–885 (2005).
38. Douglas, R.J., Mahowald, M., Martin, K.A. & Stratford, K.J. The role of synapses in cortical computation. *J. Neurocytol.* **25**, 893–911 (1996).
39. Mongillo, G., Amit, D.J. & Brunel, N. Retrospective and prospective persistent activity induced by Hebbian learning in a recurrent cortical network. *Eur. J. Neurosci.* **18**, 2011–2024 (2003).
40. McCormick, D.A. Brain calculus: neural integration and persistent activity. *Nat. Neurosci.* **4**, 113–114 (2001).
41. Gao, W.J., Krimer, L.S. & Goldman-Rakic, P.S. Presynaptic regulation of recurrent excitation by D1 receptors in prefrontal circuits. *Proc. Natl. Acad. Sci. USA* **98**, 295–300 (2001).
42. Fisher, S.A., Fischer, T.M. & Carew, T.J. Multiple overlapping processes underlying short-term synaptic enhancement. *Trends Neurosci.* **20**, 170–177 (1997).
43. Magleby, K.L. Short-term changes in synaptic efficacy. *Synaptic Function* (eds Edelman, G.M., Gall, W.E. & Cowan, W.M.) 21–56 (Wiley, New York, 1987).
44. Larkum, M.E., Kaiser, K.M. & Sakmann, B. Calcium electrogenesis in distal apical dendrites of layer 5 pyramidal cells at a critical frequency of back-propagating action potentials. *Proc. Natl. Acad. Sci. USA* **96**, 14600–14604 (1999).